Bioprocess Biosyst Eng
DOI 10.1007/s00449-013-1034-z

ORIGINAL PAPER

A label-free immunosensor for determination of salbutamol based on localized surface plasmon resonance biosensing

Ziren Yan · Tingting Hu · Wenying Guo · Anping Deng · Junwei Di

Received: 8 June 2013 / Accepted: 2 August 2013

Abstract We developed a localized surface plasmon resonance (LSPR)-based label-free optical biosensor for detection of salbutamol (Sal). Hollow gold nanoparticles (HGNs) which deposited on transparent indium tin oxide (ITO) film coated glass was used to sensing platform. Antibody against Sal was immobilized on HGN surface to recognize the target Sal molecules. Thus, the change of LSPR peak was proportional to the concentration of Sal in the solution. The experimental results demonstrated that the LSPR immunosensor possessed a good sensitivity and a high selectivity for Sal. The detection range for Sal was from 0.05 to 0.8 μg/mL with a correlation coefficient of 0.996. The biosensor was applied for the detection for Sal in spiked animal feed and pork liver samples, and the recoveries were in the range of 97–105 %. Therefore, it is expected that this approach may offer a new method in designing label-free LSPR immunosensor for detection of small molecules.

Keywords Salbutamol · Immunosensor · Localized surface plasmon resonance · Hollow gold nanostructures

Introduction

The phenomenon of localized surface plasmon resonance (LSPR) associated with noble metal nanostructures has been attracted great attention from the bioanalytical applications [1–5]. Recently, LSPR-based nanosensors have been developed to complement the surface plasmon resonance (SPR) sensors [5]. The LSPR peak wavelength of noble metal nanoparticles (especially silver and gold) is very sensitive to their surface-bound molecules and the surrounding environment. The refractive index (RI) change in the environment near noble nanoparticles is the basis of LSPR sensing. Specially, the LSPR peak changes can be obtained by recording the absorption spectroscopy of metal nanoparticles immobilized on glass substrate. Therefore, a LSPR combined with a basic UV–visible spectrophotometer has been developed for the simple and rapid sensing method.

The selectivity of a LSPR-based sensing is obtained by the immobilization of molecules on the nanoparticle surface that target specific biological relevant species from solutions. Many LSPR biosensors based on metal nanoparticles had been developed for detection of large biomolecules, such as DNA and proteins [6–9]. For example, antibody–antigen binding is the fundamental phenomenon in the field of biochemistry and biology. Thus, an antibody–antigen binding pair has often been employed in high selective bioassays. Therefore, many label-free immunoassay based on LSPR biosensors have been reported [10–12]. Moreover, label-free detection system has a high probability for developing more convenient bioassay process than the conventional ones because of avoiding the labeling procedure. This is very important for routine field analyses. However, detection of small organic molecules based on LSPR immunoassay is challenge because the RI changes induced by small molecules are lower than that by large biomolecules.

It is well known that the RI sensitivity of gold nanoparticles is strongly dependent upon the

Z. Yan · T. Hu · W. Guo · A. Deng · J. Di (✉)
The Key Lab of Health Chemistry and Molecular Diagnosis of Suzhou, College of Chemistry, Chemical Engineering and Material Science, Soochow University, Suzhou 215123, Jiangsu, People's Republic of China
e-mail: djw@suda.edu.cn

Published online: 10 August 2013

composition, shape, and size of metal nanoparticles. Miller and Lazarides [13] reported that the RI sensitivity of gold nanoparticles increased with the red-shifting LSPR peak. In other words, LSPR peak in the near-infra region (NIR) is beneficial for detection because of its larger red shift, as compared with the visible region when changes in the local dielectric environment on nanoparticle surfaces occur. Hollow gold nanoshells (HGNs) exhibit an apparent red shift of their LSPR peak relative to that of solid gold nanostructures [14, 15]. Thus, the NIR LSPR peak of HGNs provides much more RI sensitivity than that of solid gold or silver nanoparticles [16–18].

Salbutamol (Sal), [1-(4-hydroxy-3-hydroxymethylphenyl)-2-(tbutylamino) ethanol], is a β2-adrenergic receptor agonist. It is primarily used in the treatment of bronchial asthma and other forms of allergic airway disease in human being. Moreover, since Sal can reduce fat deposition in cattle, sheep, pigs, and poultry, it was abused as a growth promoter and fattening agent [19]. However, the residues of Sal which accumulated in animal tissues can cause symptoms of serious poisoning in human [20]. Thus, in many countries, application of Sal has been banned as a repartitioning agent in meat-producing animals [21]. Although many analytical methods, such as spectrophotometry [22, 23], high-performance liquid chromatograph (HPLC) [24, 25], capillary electrophoresis [26], electrogenerated chemiluminescence [27], electrochemical method [28], and immunosensor [29] have been developed for Sal detection, many of these techniques require expensive instrumentation or time-consuming.

In our previous paper, we reported the fabrication of gold nanoparticles on transparent indium tin oxide (ITO) glass surface and its application for construction of label-free LSPR biosensor [30]. Here, we combine the high RI sensitivity of HGNs with the advantage of immunological technique to construct a label-free and reagentless LSPR biosensor for detecting Sal. Scheme 1 shows the preparation process of immunosensor. Silver nanoparticles are deposited directly on ITO substrate by electrochemical method. Then HGNs are formed by replacement reaction with $HAuCl_4$. Antibody (Ab) against Sal can be absorbed on the gold surface because of clean without organic ligands. The analytical performance of resulting biosensor was investigated. It is possible to use the label-free LSPR biosensors for field analysis.

Experimental

Materials

Indium tin oxide glass (1.1 mm of thickness, less than 100 Ω) was obtained from Suzhou NSG Electronics Co., Ltd. (Suzhou, China). Antibody (Ab) against Sal was prepared by our laboratory. All reagents were used as received without further purification. Tetrachloroauric acid ($HAuCl_4$) and silver nitrate ($AgNO_3$) were purchased from Guoyao Chemical Reagent Co, Ltd., China. A phosphate buffer solution (PBS, pH 7.0) was prepared using 0.05 mol/L of NaH_2PO_4 and 0.05 mol/L of Na_2HPO_4 solution. All chemicals were of analytical grade. Double-distilled deionized water was used in all experiments.

Apparatus

All electrochemical depositions were performed using CHI 830 electrochemical workstation (CH Instruments, Shanghai, China). A conventional three-electrode system was used which consists of a saturated calomel electrode (SCE) as a reference electrode, a bare ITO electrode as a working electrode, and a platinum wire as a counter electrode. The absorption spectra were measured on a TU-2810 spectrophotometer (Beijing Purkinje General Instrument Co., Ltd.). The surface morphology of metal nanoparticles was recorded by a dimension 3100 model atomic force microscope (AFM) (Veeco, Santa Barbara, CA) equipped with a nanoscope IV controller (digital instruments). Scanning electron microscopy (SEM) image was obtained using S-4700 scanning electron microscope (Hitachi, Japan).

Preparation of HGNs on ITO substrate surface

The HGNs were prepared according to our previous report with some modification [18]. Briefly, The ITO (0.6×3.0 cm^2) strip was cleaned using NH_3–H_2O (1:20), ethanol, and distilled water for 10 min sequentially in an ultrasonic

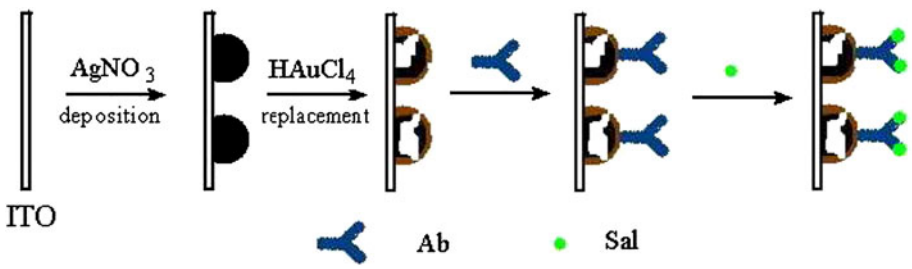

Scheme 1 Illustration of the preparation process of label-free immunosensor

bath. The electrolyte consisted of 0.2 mmol/L $AgNO_3$ and 0.3 mol/L KNO_3 solution was bubbled by high purity N_2 for at least 10 min prior to electrolysis and maintained under N_2 atmosphere during experiments. The AgNPs were electrodeposited onto the ITO electrodes at 30 °C by applying a cyclic voltammogram (CV) in the potential range −0.2 to −0.5 V at 0.05 V/s for 100 cycles. After rinsing with water, the slides were incubated in 0.02 mM $HAuCl_4$ solution for 20 min at 50 °C. We defined this strip as ITO/HGNs.

Fabrication of the biosensor

Because the gold surface of HGNs is already clean with no organic ligands, proteins can be directly adsorbed on it. The Sal biosensor was fabricated by immersing ITO/HGNs strips in 7 μg/mL of Ab and PBS solution (pH 7.0) for 10 h at 4 °C. Those strips were throughout rinsed with water and then ready for use.

Detection of Sal

All LSPR bands were monitored against a bare ITO glass as a reference. The immunosensor was first rinsed throughout by water and dried by nitrogen gas. Then the LSPR band was recorded. Next, this immunosensor was incubated in Sal sample and phosphate-buffer solution (pH 7.0) for 30 min at 30 °C. After rinsing and drying, the LSPR band was recorded again. Therefore, the change of LSPR peak of immunosensor was obtained for detection of Sal concentration.

Sample preparation

Pig complex feed was purchased from a local feedstuff market (Suzhou). Pork liver and milk were obtained from a local supermarket (Suzhou). The samples, 3.0 g ground pig complex feed, 3.0 g of minced and homogeneous mixed pork liver, and 5.0 mL of milk were transferred to their respective glass-stoppered glass tubes. Then, 0.1 mol/L HCl was added into the tube to 10 mL tick mark. The samples were treated in ultrasonic vibration system for 0.5 h and kept at room temperature overnight. Next, they were ultrasonic-mixed for 15 min, and centrifuged at 12,000 rpm. Finally, the clear supernates were collected and adjusted to near pH 7.0 for detection.

Results and discussion

Characterization of HGNs onto transparent ITO substrate

HGNs immobilized on transparent ITO substrate surface were prepared by the reaction of aqueous $HAuCl_4$ solutions with AgNPs as templates [18]. Figure 1 presents a typical AFM image and of the resulting HGNs. The prepared HGNs were quasi-hemispherical onto the substrate surface. The diameter of the HGNs ranged from 60 to 90 nm. The results were consistent with that obtained from SEM image (Fig. 2). From the cyclic voltammograms of the AgNPs and HGNs deposited ITO electrodes, it indicated that gold was deposited on the electrode and silver was not dissolved completely. The wall thickness of HGNs is approximately one-tenth of the radius of the template AgNPs even if silver templates are completely converted to gold shell [16, 18]. Thus, the thickness of gold shell was estimated to be ~3 nm.

Curve a in Fig. 3 shows the absorption spectrum of HGNs. Its plasmon resonance was located at ~800 nm, indicating formation of hollow gold nanostructures. This is consistent with the previous reports [16, 18]. The RI sensitivity was determined by recording the absorption spectra of HGNs in media with different solvents. The LSPR spectra of HGNs deposited on transparent ITO substrate were measured in ethanol ($n = 1.362$), cyclohexane ($n = 1.426$), chloroform ($n = 1.4467$), and carbon tetrachloride ($n = 1.4604$). As seen in Fig. 3a, the LSPR peak red shifted with increasing RI value. The LSPR peak wavelength was linear with the respective RI (Fig. 3b). Thus, the sensitivity was evaluated from the slope to be

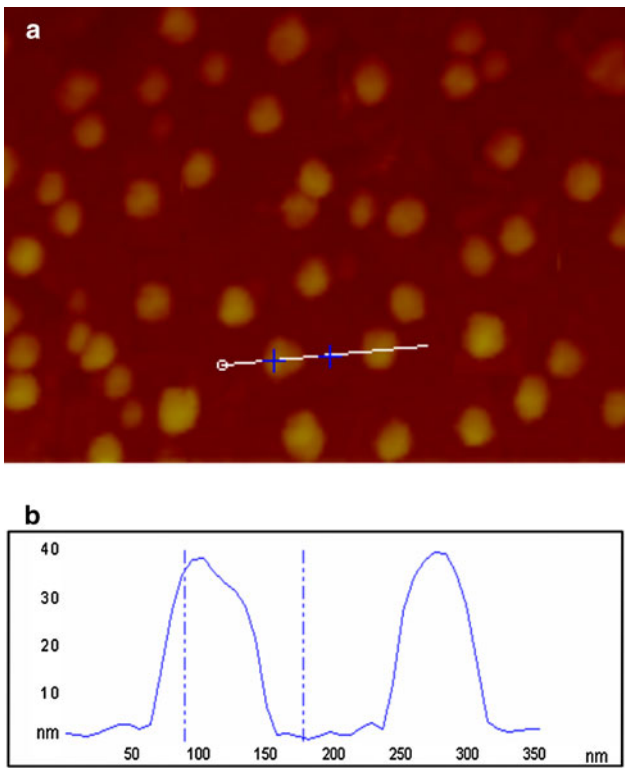

Fig. 1 A typical AFM image of HGNs grown on ITO substrate (**a**) and the section analysis of the HGNs (**b**)

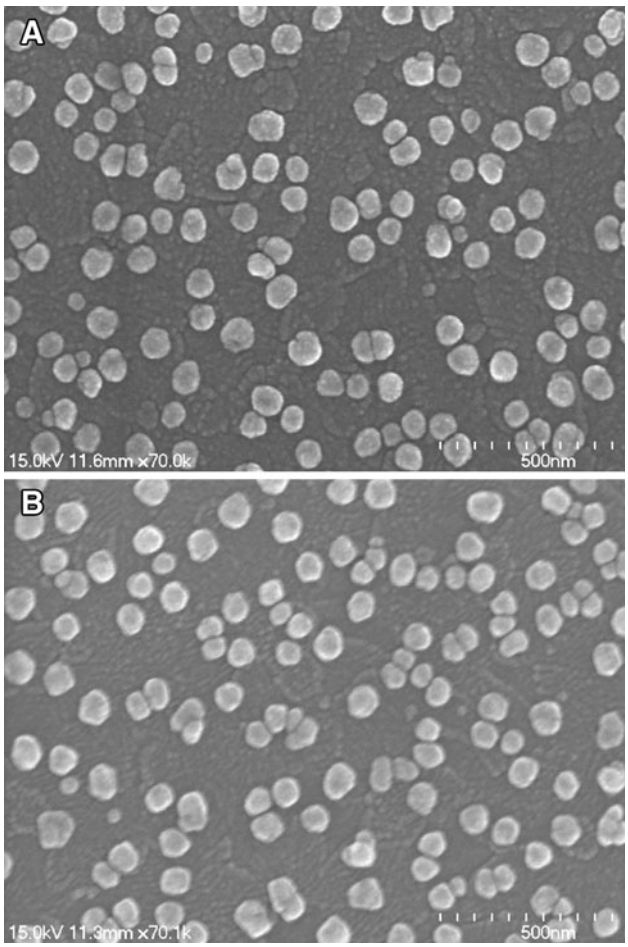

Fig. 2 SEM image of AgNPs (**a**) and HGNs (**b**) deposited on ITO substrate

276 nm/RIU, which was more sensitive than that of 245 nm/RIU at 705 nm for twin-linked GNPs [30] and 252 nm/RIU at 700 nm for gold nanorods [31].

Determination of Sal

The principle of the LSPR biosensor for detecting Sal is immunological reaction. Antibody responding to Sal was first immobilized on HGN surface. It could selectively react with Sal molecules, which resulted in changes of RI surrounded the HGNs. As a result, the LSPR peak of HGNs red-shifted with increasing the concentration of Sal. Based on this principle, a label-free LSPR biosensor for Sal with simple method and high selectivity is designed.

Since the surface of HGNs prepared by galvanic replacement reaction was free of organic stabilizers, protein molecules could be adsorbed directly on the gold surface. The adsorption of protein can induce the red-shift of HGN LSPR band. Thus, we could conveniently follow the Ab adsorption on the HGN surface using the spectroscopic method. Figure 4 shows the LSPR peak wavelength

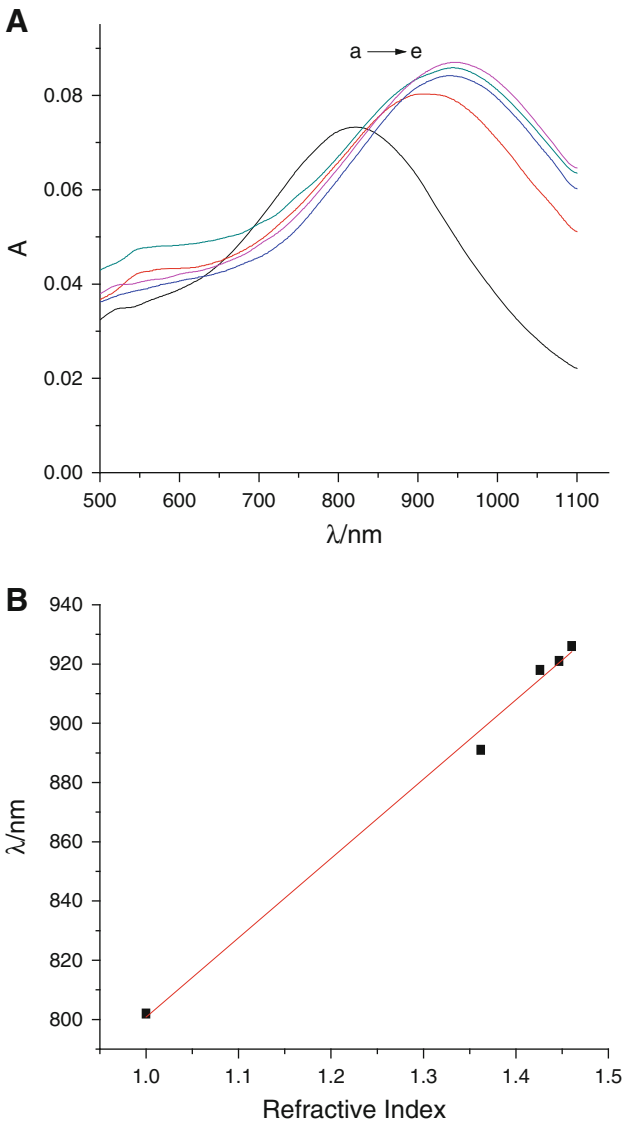

Fig. 3 UV–visible absorption spectra of the HGN platform in air, ethanol, cycloexane, chloroform, and carbon tetrachloride medium, respectively (**A**), and calibration curve of the LSPR peak on the RI for HGN sensing platform

shift as a function of Ab concentration and time. The red shift wavelength increased with increasing the concentration of Ab at first, and then reached a plateau over the concentration of 5 μg/mL. This suggested that the saturated adsorption of Sal occurred. The LSPR peak also red-shifted with increasing the incubation time and reached adsorption equilibrium over 8 h. Therefore, we selected incubation in 7 g/mL of anti-Sal-IgG solution for ~10 h in the next experiments.

The next step was the actual bioassay and involved the binding of Sal onto the Ab surface. This affinity interaction yielded a further red shift of the LSPR peak, which was the basis of the LSPR biosensor. Figure 5 displays the LSPR peak changes with the incubation time in Sal solution at

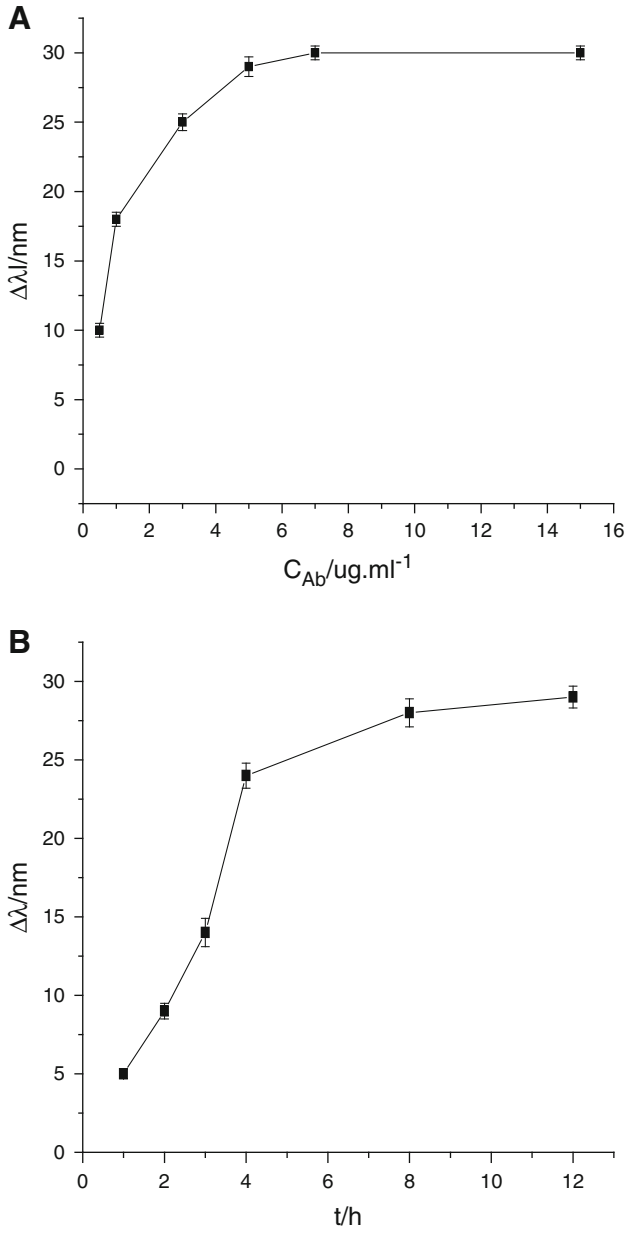

Fig. 4 LSPR peak wavelength shift of HGNs vs concentration of Ab (**a**) and incubation time (**b**)

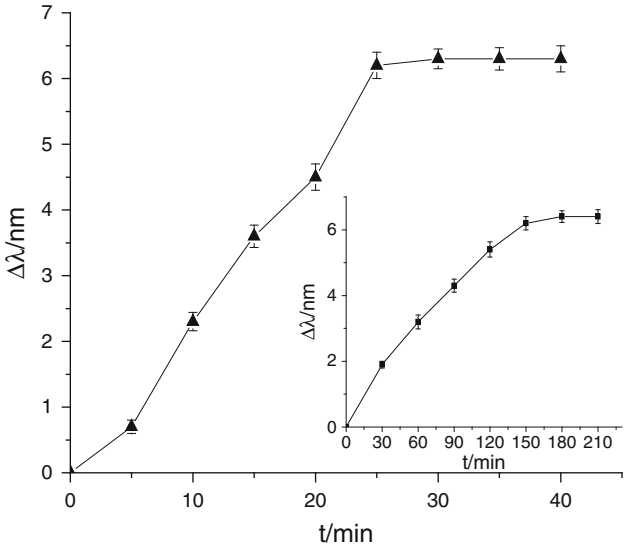

Fig. 5 LSPR peak wavelength shift of HGNs immobilized Ab vs incubation time in 0.5 μg/mL of Sal solution at 30 °C. *Inset* incubation at 4 °C

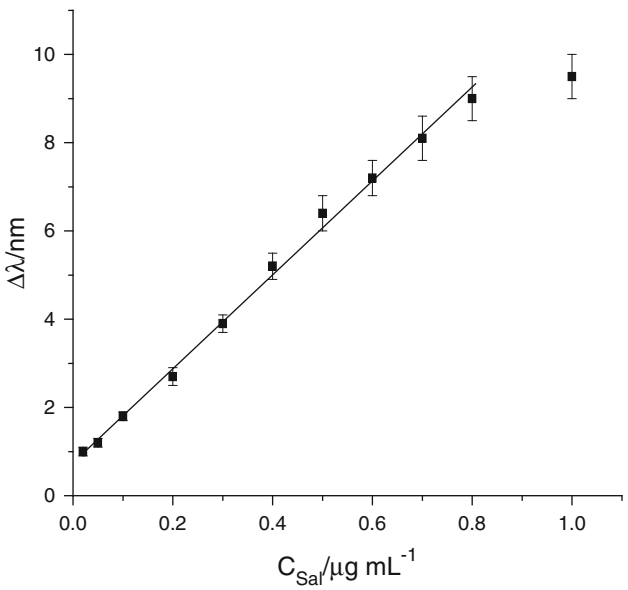

Fig. 6 A calibration curve for detection of Sal in solution at different concentrations

different temperature. During the course of binding, there was a red shift in the LSPR peak. The red shift reached plateau when the incubation time was over 25 min at 30 °C. In the control experiments, no marked changes (∼1 nm) were observed in the absorption spectra before or after incubation of biosensor in the buffer solution. For comparison, the red shift vs incubation time at 4 °C is shown in inset of Fig. 5. The peak shift reached maximum after the incubation time was over 2.5 h. Thus, incubation time of 30 min at 30 °C was used in the next experiments.

Figure 6 shows the red shift wavelength of the sensor to various concentration of Sal solution. These data indicate that the biosensor was in good linear relationship with Sal concentration. The calibration range of Sal concentration was from 0.05 to 0.8 μg/mL ($R = 0.996$), and the limit of determination for Sal was estimated as 0.02 μg/mL. This value exhibited rather high sensitivity when compared with those reported for the detection Sal in the range of 0.5–5.0 μg/mL for spectrophotometry [23], 0.1–2 μg/mL for voltammetry [28], 10–50 μg/mL for capillary electrophoresis [26], 2.4–23.8 μg/mL for electrogenerated

Table 1 Determination of Sal in spiked real samples ($n = 3$)

Sample	Spiked (μg/mL)	Found (μg/mL)	RSD (%)	Recovery (%)
Animal feed	0.20	0.210	3.4	105
Pork liver	0.20	0.193	4.1	97
Milk	0.20	0.202	2.0	101

chemiluminescence [27], and 0.025–0.3 μg/mL for HPLC [24]. Moreover, no significant changes in the response were observed for more than 30 days after the sensor were stored at 4 °C. Therefore, the biosensor has good stability for practical application.

The selectivity of the LSPR biosensor was evaluated using standard solution. Based on the optimized methods described above, the changes of LSPR peak were measured before and after being spiked with interfering substances. The changes were less than 1 nm for 10 μg/mL of chloromycetin, 10 μg/mL of ractopamine, and 2 μg/mL of bovine serum albumin (BSA). If necessary, the LSPR biosensor can be blocked by BSA after the antibody step for further reducing a significant amount of nonspecific binding. Because the surface of metal nanostructures was covered almost completely by proteins (Ab and/or BSA), the interference come from the nonspecific absorption could be avoided. The high selectively of the biosensor comes from the particular interaction between the antibody–antigen pair reaction. However, 0.5 μg/mL of clenbuterol yielded red shift of 6 nm, indicating that clenbuterol would induce similar changes with Sal. Note that clenbuterol is another β2-adrenergic receptor agonist which is also banned as a repartitioning agent in meat-producing animals. Therefore, the selectivity of the LSPR biosensor was acceptable for detecting Sal.

To further investigate the reliability of the detection method, the developed LSPR biosensor was applied to Sal determination in spiked animal feed, pork liver, and milk samples. The content of Sal was not found in the samples by directly detecting. Table 1 shows the measurement results obtained from the detection of three replicates of the samples. Satisfactory recoveries for Sal were obtained, suggesting the potential of the developed LSPR biosensor for the detection of Sal in biological samples.

Conclusion

A simple strategy for the fabrication of an LSPR sensing system for sensitive Sal detection is described. This method combines the advantages of hollow gold nanostructures as sensing platform with immunological technique. The LSPR immunosensor is label-free, reagentless, with high sensitivity and good selectivity, without requiring expensive equipment. More significantly, it is fairly easy to generalize this strategy to immobilize different antibodies against drug. Therefore, it is expected that this approach may offer a method in constructing label-free LSPR immunosensor for sensitive and selective detection of small molecules.

Acknowledgments This work was financially supported by the National Natural Science Foundation of China (No. 21075086), the Project of Scientific and Technologic Infrastructure of Suzhou (SZS201207) and the Priority Academic Program Development of Jiangsu Higher Education Institutions.

References

1. Mayer KM, Hafner JH (2011) Localized surface plasmon resonance sensors. Chem Rev 111:3828–3857
2. Stewart ME, Anderton CR, Thompson LB, Maria J, Gray SK, Rogers JA, Nuzzo RG (2008) Nanostructured plasmonic sensors. Chem Rev 108:494–521
3. Chen H, Ming T, Zhao L, Wang F, Sun L, Wang J, Yan C (2010) Plasmon—molecule interactions. Nano Today 5:494–505
4. Sepúlveda B, Angelomé PC, Lechuga LM, Liz-Marzán LM (2009) LSPR-based nanobiosensors. Nano Today 4:244–251
5. Shon Y, Choi HY, Guerrero MS, Kwon C (2009) Preparation of nanostructured film arrays for transmission localized surface plasmon sensing. Plasmonics 4:95–105
6. Endo T, Kerman K, Nagatani N, Takamura Y, Tamiya E (2005) Label-free detection of peptide nucleic acid-DNA hybridization using localized surface plasmon resonance based optical biosensor. Anal Chem 77:6976–6984
7. Nath N, Chilkoti A (2004) Label-free biosensing by surface plasmon resonance of nanoparticles on glass: optimization of nanoparticle size. Anal Chem 76:5370–5378
8. Li C, Wu C, Zheng J, Lai J, Zhang C, Zhao Y (2010) LSPR sensing of molecular biothiols based on noncoupled gold nanorods. Langmuir 26:9130–9135
9. Vestergaard M, Kerman K, Kim D, Hiep HM, Tamiya E (2008) Detection of Alzheimer's tau protein using localized surface plasmon resonance-based immunochip. Talanta 74:1038–1042
10. Wang C, Ma Z, Wang T, Su Z (2006) Synthesis, assembly, and biofunctionalization of silica-coated gold nanorods for colorimetric biosensing. Adv Funct Mater 16:1673–1678
11. Mayer KM, Lee S, Liao H, Rostro BC, Fuentes A, Scully PT, Nehl CL, Hafner JH (2008) A label-free immunoassay based upon localized surface plasmon resonance of gold nanorods. ACS Nano 2:687–692
12. Fan M, Thompson M, Andrade ML, Brolo AG (2010) Silver nanoparticles on a plastic platform for localized surface plasmon resonance biosensing. Anal Chem 82:350–6352
13. Miller MM, Lazarides AA (2005) Sensitivity of metal nanoparticle surface plasmon resonance to the dielectric environment. J Phys Chem B 109:21556–21565
14. Wan D, Chen H, Lin Y, Chuang S, Shieh J, Chen S (2009) Using spectroscopic ellipsometry to characterize and apply the optical constants of hollow gold nanoparticles. ACS Nano 3:960–970

15. Vongsavat V, Vittur BM, Bryan WW, Kim J, Lee TR (2011) Ultrasmall hollow gold_silver nanoshells with extinctions strongly red-shifted to the near-infrared. ACS Appl Mater Interfaces 3:3616–3624
16. Sun Y, Xia Y (2002) Increased sensitivity of surface plasmon resonance of gold nanoshells compared to that of gold solid colloids in response to environmental changes. Anal Chem 74:5297–5305
17. Wang Y, Qian W, Tan Y, Ding S (2008) A label-free biosensor based on gold nanoshell monolayers for monitoring biomolecular interactions in diluted whole blood. Biosens Bioelectron 23:1166–1170
18. Hu T, Lin Y, Yan J, Di J (2013) Synthesis of hollow gold nanoparticles on the surface of indium tin oxide glass and their application for plasmonic biosensor. Spectrochim Acta A Mol Biomol Spectrosc 110:72–77
19. Sheu S, Lei Y, Tai Y, Chang T, Kuo T (2009) Screening of salbutamol residues in swine meat and animal feed by an enzyme immunoassay in Taiwan. Anal Chim Acta 654:148–153
20. Libretto SE (1994) A review of the toxicology of salbutamol (albuterol). Arch Toxicol 68:213–216
21. Chai C, Liu G, Li F, Liu X, Yao B, Wang L (2010) Towards the development of a portable sensor based on a molecularly imprinted membrane for the rapid determination of salbutamol in pig urine. Anal Chim Acta 675:185–190
22. Mohamed GG, Khalil SM, Zayed MA, El-Shall MAE (2002) 2,6-Dichloroquinone chlorimide and 7,7,8,8-tetracyanoquinodimethane reagents for the spectrophotometric determination of salbutamol in pure and dosage forms. J Pharmaceut Biomed 28:1127–1133
23. Basavaiah K, Prameela HC (2003) Three useful bromimetric methods for the determination of salbutamol sulfate. Anal Bioanal Chem 376:879–883
24. Mazhara SHRA, Chrystyn H (2009) New HPLC assay for urinary salbutamol concentrations in samples collected post-inhalation. J Pharmaceut Biomed 50:175–182
25. Zhang J, Xu Y, Di X, Wu M (2006) Quantitation of salbutamol in human urine by liquid chromatography–electrospray ionization mass spectrometry. J Chromatogr B 831:328–332
26. Mikuš P, Valášková I, Havráánek E (2005) Determination of salbutamol in pharmaceuticals by capillary electrophoresis. Arch Pharm Chem Life Sci 338:498–501
27. Lindino CA, Bulhões LOS (2007) Determination of fenoterol and salbutamol in pharmaceutical formulations by electrogenerated chemiluminescence. Talanta 72:1746–1751
28. Goyal RN, Kaur D, Singh SP, Pandey AK (2008) Effect of graphite and metallic impurities of C60 fullerene on determination of salbutamol in biological fluids. Talanta 75:63–69
29. Huang J, Lin Q, Zhang X, He X, Xing X, Lian W, Zuo M, Zhang Q (2011) Electrochemical immunosensor based on polyaniline/poly (acrylic acid) and Au-hybrid graphene nanocomposite for sensitivity enhanced detection of salbutamol. Food Res Int 44:92–97
30. Deng J, Song Y, Wang Y, Di J (2010) Label-free optical biosensor based on localized surface plasmon resonance of twin-linked gold nanoparticles electrodeposited on ITO glass. Biosens Bioelectron 26:615–619
31. Marinakos SM, Chen S, Chilkoti A (2007) Plasmonic detection of a model analyte in serum by a gold nanorod. Anal Chem 79:5278–5283